JOURNAL OF PROPULSION AND POWER
Vol. 9, No. 1, Jan.–Feb. 1993

Effects of Injector Geometry on Scramjet Combustor Performance

Nobuo Chinzei,* Tomoyuki Komuro,† Kenji Kudou,‡ Atsuo Murakami,† Kouichiro Tani,† Goro Masuya,§ and Yoshio Wakamatsu¶
National Aerospace Laboratory, Miyagi 981-15, Japan

An experiment was conducted to investigate the effect of injector/combustor geometry on combustion-induced peak wall pressure and associated upstream influence, as well as on mixing/combustion characteristics at an entrance Mach number of 2.5. The length of the constant area section downstream of injection orifices had a strong influence on the above-mentioned characteristics. However, the sweep of the rearward-facing steps on both side walls had little effect on these characteristics, nor did reversing them have any effect. The peak wall pressure and the length of the upstream influence agreed qualitatively with predictions of an analytical model and an empirical formula developed at Johns Hopkins University. Fuel jets injected from the model with the longest constant area section and the fuel equivalence ratio of unity, coalesced at a very early stage downstream of the fuel injection orifices. This coalescence led to a decrease in mixing rate downstream, despite the higher degree of mixing near the injection orifices. The combustion efficiencies were higher than those obtained at NASA Langley in the upstream region due to the higher mixing rate near the injection orifices.

Nomenclature

A = cross-sectional area
C = mass concentration
H = combustor entrance height
h = rearward-facing step height
h_t = total enthalpy
L = combustor length measured from the step
L_c = length of constant area section
l_i = distance of the upstream influence
m = mass flow rate
p = pressure
p_{wa} = wall pressure at the point where it diverges from that of the noninjection case
T = temperature
u = velocity in x direction
W = molecular weight
x, y, z = Cartesian coordinates, (Fig. 1)
α = sweep angle of the step
γ = specific heat ratio
δh_t = increment of h_t due to combustion
δT_t = increment of T_t due to combustion
η_c = combustion efficiency
η_m = mixing efficiency
ρ = density
Φ = Eqs. (4a) and (4b)
Φ' = Eqs. (3a) and (3b)
ϕ = overall fuel equivalence ratio before burning
ϕ' = local fuel equivalence ratio at the hypothetical state before burning

Subscripts
a = air or vitiated air
b = fuel burnt
f = fuel before burning
max = maximum
t = total or stagnation
w = wall

Received Oct. 31, 1991; revision received July 2, 1992; accepted for publication July 29, 1992.

*Head, Ramjet Performance Section, Kakuda Research Center.
†Researcher, Ramjet Performance Section, Kakuda Research Center.
‡Senior Researcher, Kakuda Research Center.
§Senior Researcher, Kakuda Research Center. Member AIAA.
¶Head, Ramjet Structure Section, Kakuda Research Center.

Introduction

AMONG various components of the scramjet engines, the combustor presents the most difficult problems. It is in this component where fuel should be thoroughly mixed with air and where reliable ignition and stable flame-holding should be achieved in an extremely high velocity stream. Previous experimental works in this field can be classified into three categories: 1) ignition/flame-holding, 2) mixing/combustion, and 3) combustion mode. Since the present study focuses on the effect of injector/combustor geometry on mixing/combustion performances, the research relevant to the present study as reported in the literature is briefly reviewed first.

Anderson et al.[1] investigated the combustor behavior with entrance Mach numbers of 1.3 and 1.7 by using a unique model simulating the center strut of the NASA-Langley's airframe integrated scramjet. They observed that the swept-step caused nonuniform mass flux distribution of the test gas and also found that there were no significant disturbances ahead of the step even with stoichiometric fuel injection, implying a suppression effect of the swept-step. Diskin and Northam[2] examined the effects of scale and geometric parameters on the combustor performances with an entrance Mach number of 2.0. The length of the constant area section downstream of the fuel injector was found to have a strong effect on both the combustion and the amount of fuel injected without resulting in upstream interaction. The addition of the constant area section acted also as a combustion stabilizer by causing higher pressure.

Billig and Dugger[3] at the Johns Hopkins University, Applied Physics Laboratory (JHU-APL) developed an analytical method to predict the strength of a precombustion shock appearing at the combustor entrance caused by phenomena occurring in the combustor. The wall pressure distribution predicted by this method agreed with the experimental results reasonably well. In relation to this method, the upstream influence of the precombustion shock has long been one of the primary concerns of the JHU-APL group. In their engine tests, Billig et al.[4] experienced forward recirculation of the fuel-air mixture, leading to inlet unstart and, in the worst case, to burning outside the inlet cowl. This was mitigated by

adding an isolator duct between the inlet and the combustor. The isolator, however, is a source of total pressure loss, especially in the supersonic flow. In order to determine the optimum length of the isolator, they introduced a semiempirical model describing wall pressure distribution. Waltrup and Billig[5] later modified this model by conducting tests on a nonreacting cylindrical duct with downstream throttling to simulate combustion-induced compression.[6] The adequacy of this model for a rectangular duct was confirmed by Bement et al.[7]

Researchers in countries other than the United States have also contributed to the field. Masuya et al.[8] conducted an experiment on the supersonic combustion mode in air breathing rocket combustors with entrance Mach numbers of 1.7–2.2. They observed that mixing and combustion performances were much poorer in a supersonic combustor than in a subsonic one. When a short constant area section was attached at the entrance of the diverging combustor, mixing performance was greatly improved, and dual-mode combustion was attained, that is, the flow immediately downstream of the entrance was subsonic, but soon became supersonic. Komuro et al.[9,10] conducted tests on a cylindrical combustor with an entrance Mach number of 2.5. By increasing the fuel equivalence ratio, the combustion mode changed from supersonic to subsonic. They also observed a drastic difference between sub- and supersonic combustions in fuel distribution over the combustor exit cross section. Avrashkov et al.[11] examined the effect of combustor geometry with an entrance Mach number of 2.5 by using kerosene as fuel. They found that the peak pressure near the combustor entrance increased when the divergence in that portion decreased, a result similar to that by Diskin and Northam.[2]

Despite comprehensive studies described above, there still remain important characteristics of the supersonic combustors to be clarified. Some of them are as follows: 1) the effect of the length of constant area section in detail; 2) mixing improvement by reversing the swept-step on the two side walls due to nonuniform flow; 3) the effects of the sweep and the constant area length on the extent of upstream propagation of combustion-induced pressure waves; and 4) applicability of the analytical method for calculating the precombustion shock strength and the empirical formula for the upstream influence proposed by the JHU-APL group for various configurations.

The present experiment was conducted to clarify the above-mentioned issues. Five types of injector/combustor models were tested. By measuring wall pressure distributions, combustion-induced peak wall pressure, and the associated upstream influence as well as on mixing/combustion characteristics were examined and compared with the formula developed at JHU-APL.[3,5] The contours of the fuel equivalence ratio over the cross section were obtained from Pitot pressure and gas composition measurements. They were compared with each other to identify the difference of mixing characteristics and were integrated to obtain mixing/combustion efficiencies. The mixing/combustion efficiencies obtained with the present models are compared with those obtained at NASA-Langley.[2,12]

Experimental Apparatus

Air Heater and Nozzle

Most of the hardware used is the same as that used by Sato et al.[13,14] and by Masuya et al.[15] in tests of auto- and forced ignition. Figure 1 shows a typical experimental setup. A hydrogen vitiation air heater[16] was used for simulating high temperature air entering the supersonic combustor. The test gas nominally contained the same volumetric fraction of 21% unreacted oxygen as that of air. The maximum values of stagnation temperature and pressure of the test gas, T_{ta} and p_{ta}, were 2500 K and 1.0 MPa, respectively. The maximum total temperature corresponds to a flight condition of Mach 7.5.

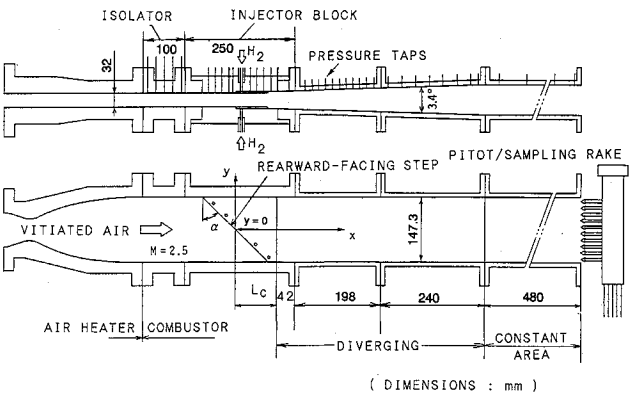

Fig. 1 Typical experimental setup.

Table 1 Injector block models

Model	α, deg (Sweep angle)	L_c, mm (Constant area section)
N1	0	96
N2	0	96 (left) 22 (right)
N3	0	22
S1	+45	96[a]
S2	+45 (left) −45 (right)	96[a]

[a]For the swept and reversed-swept step, the length of the constant height section is measured along the line of $y = 0$.

Downstream of the heater, a two-dimensional Laval nozzle, the design of which was based on the method of characteristics, was attached to accelerate the test gas to supersonic velocity. The nominal Mach number at the nozzle exit (i.e., at the combustor entrance) was 2.5. The nozzle exit had a cross section 32-mm in height ($=H$) by 147.3-mm in width. The heater and the nozzle were cooled by a heat-sink. The hardware was made of copper, except for the heater housing which was made of carbon steel. In order to prevent the combustion-induced pressure waves in the test section from propagating upstream into the nozzle, a constant area isolator duct 100-mm long was placed between the nozzle and the combustor. The boundary-layer thickness at the isolator exit, measured by a smaller Pitot probe rake to be described later, was 10 mm on the average.

Combustor and Fuel Injectors

In order to identify the position inside the combustor in the rest of this article, Cartesian coordinates with the x axis parallel to the main stream, the y axis parallel to the side plate, and the z axis normal to them are introduced as shown in Fig. 1.

The combustor consisted of an injector block and downstream ducts. Its entrance had a rectangular cross section of the same size as the nozzle exit and the isolator. The width was kept constant all the way up to the combustor exit. Five different pairs of replaceable injector blocks with a length of 250 mm were tested. In designing the injectors, major dimensions were determined by referring to a "recipe" recommended by NASA Langley.[2] All of these injector blocks had rearward-facing steps with a height, h, equal to $H/10$ (3.2 mm) for flame-holding and suppressing upstream propagation of combustion-induced pressure waves.

Differences in the injector blocks were the sweep angle a of the step and the length of the constant area section L_c behind it as shown in Table 1 and Fig. 2. The location of the step at $y = 0$ on each side wall coincided at $x = 0$ for all the models, except model N2 which had the steps on the two side walls staggered in the x direction with each other. The objective in using the models N1, N2, and N3 was to elucidate

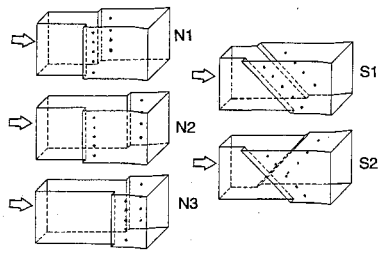

Fig. 2 Schematics of injector block models.

the effect of the length of the constant area section, while models S1 and S2 were used to reduce the combustion-induced upstream influence as implied by Anderson et al.[1] and to examine the effect of swept-steps on mixing characteristics.

Gaseous hydrogen fuel was injected perpendicularly from the side walls at sonic condition. The injection orifices were located $4h$ downstream of the step in the direction parallel to the x axis in all the cases. The spacing between them, measured perpendicularly to the x axis, was set equal to H for the optimum mixing characteristics as suggested by Anderson et al.[17] Four injection orifices with a diameter of 4 mm were drilled in one of the side walls and five orifices in the other wall. The orifices on the two side walls were staggered with each other in the y direction. The diameters of the latter orifices were 4 mm for the three central orifices and 2.5 mm for the orifices at either end in order to avoid too rich a mixture of hydrogen near the top and the bottom walls, as well as to allocate an equal amount of fuel to both walls.

The length downstream of the injector block could be varied up to 918 mm in four steps as shown in Fig. 1. These lengths corresponded to combustor lengths L defined as the distance from the step to the exit along the x axis of 138, 336, 576, and 1056 mm for models N1, N2, S1, and S2. For model N3, L were shorter than those of the other models by 74 mm, because the step was located downstream. The side plates diverged at the exit of the constant area section with a half-angle of 1.7 deg. For the longest combustor, however, a pressure rise due to boundary layer separation induced by overexpansion of the exit stream which was discharged to the atmosphere, was observed during the earlier runs. In the later runs, therefore, the divergence angle of the end section with a length of 480 mm was kept at zero to avoid such an undesirable phenomenon. The combustor and the injector blocks were cooled by a heat-sink and made of stainless steel.

Procedures

Pressure taps were installed on the side walls at intervals of 10–20 mm. Pitot pressure measurement and gas sampling were conducted along a line parallel to the y axis by attaching a water-cooled eleven-point probe rake. The measurement was repeated several times by changing the probe rake location in the z direction under the same experimental conditions to obtain cross-sectional distributions. As stated before, the Pitot pressure profile in the boundary layer at the exit of the nozzle was also measured by another smaller uncooled probe rake to obtain its thickness. The operating duration of the vitiation air heater was 7 s, with the steady state being established about 1.5 s after the initiation. Fuel was injected mostly 3 s after the heater initiation, but at a T_{ta} value lower than around 1500 K, autoignition could not be expected.[13] For such lower T_{ta} cases, fuel was injected simultaneously with the heater initiation so that the transient high temperature produced in the heater could ignite the fuel.[9,18] Measurements of wall and Pitot pressures and gas sampling were begun 4.2 and 4.8 s after heater initiation, respectively.

From analyses of gas sampled at each probing point over the cross section, and from mass flow rate measurements of air, oxygen, and hydrogen, cross-sectional distributions of each species were obtained as follows:

In calculating these distributions, the vitiated air was assumed to be uniformly mixed and completely reacted. The validity of these assumptions was confirmed to be correct within ±15% in the certification test of the heater.[16] Thus, the local concentration of air was determined from that of nitrogen in the sampled gas. From this and the results of mass flow rate measurements for air and oxygen injected into the heater, the local concentration of oxygen at the hypothetical state before burning was determined. From the difference between the local concentration of oxygen before burning that was determined and that residual in the sample, the concentration of burnt hydrogen C_b was calculated. The local concentration of hydrogen at the hypothetical state before burning C_f was determined by adding those of the burnt hydrogen and that residual in the sample.

The mixing and combustion efficiencies, η_m and η_c, are defined as follows:

$$\eta_m = \int_A (\rho u C_f/\Phi') \left[\frac{dA}{(m_f/\Phi)}\right] \tag{1}$$

$$\eta_c = \int_A \rho u C_b \left[\frac{dA}{(m_f/\Phi)}\right] \tag{2}$$

$$\Phi' = 1 (\phi' \leq 1) \tag{3a}$$

$$\phi' (\phi' \geq 1) \tag{3b}$$

$$\Phi = 1 (\phi \leq 1) \tag{4a}$$

$$\phi (\phi \geq 1) \tag{4b}$$

Here, integrations are done over the combustor cross section. The denominator in Eqs. (1) and (2) represents the amount of fuel that would react if the mixture were uniform. The numerators in these equations are the amount of fuel that would react for η_m and that actually burnt for η_c, respectively.

Values of ρ and u in the integrals of Eqs. (1) and (2) are calculated from measured Pitot pressure and static pressure approximated by interpolation among wall pressures. The specific heat ratio and molecular weight of the gas at each point were calculated by assuming a uniform mixture consisting of the unburnt deficient reactant and the rest, each of which is under chemical equilibrium at the same pressure and temperature. In carrying out the above integration, the distribution of the velocity from the wall to the nearest probing points was approximated by the $\frac{1}{7}$th power law.

Results and Discussion

Wall Pressure Distributions

The effect of ϕ on the wall pressure distributions at the two side walls along the x axis is shown in Fig. 3 for the injector model N1 with L = 1056 mm and T_{ta} = 2000 K. The wall pressure p_w is normalized by p_{ta}. There is no significant difference between the distributions on the two side walls (shown as "$+z$" and "$-z$" in the figure, respectively). As the side walls diverged up to the exit for these runs, p_w rise abruptly near the exit due to boundary-layer separation as described earlier. The distributions show general trends common to all the cases, i.e., a peak pressure appears near the injection orifices caused by so-called "precombustion shock"[11] followed by a steep reduction. As ϕ is increased, the level of the distributions becomes higher due to the increase in heat release, and its effect propagates upstream beyond the step for ϕ greater than 0.6. The extent to which the upstream region is influenced seems to depend on the magnitude of the peak pressure. Similar behavior was observed when T_{ta} was decreased under constant ϕ. The distributions of p_w for L shorter than those in the figure were also measured up to L = 138 mm. The results were almost the same as those in

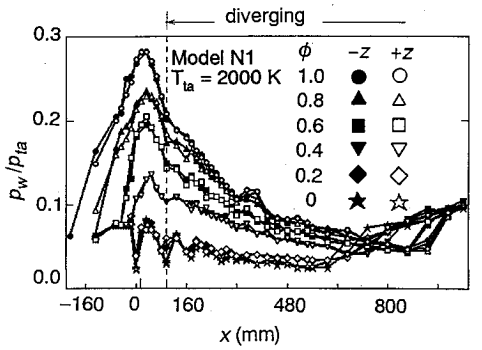

Fig. 3 Effect of ϕ on p_w distributions.

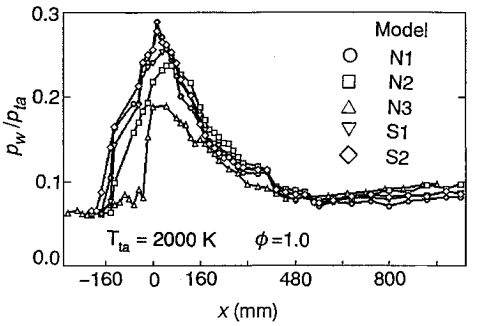

Fig. 4 Effect of injector geometry on p_w distributions.

Fig. 3, evidence of the occurrence of supersonic combustion downstream of L = 138 mm.

The wall pressure distributions at ϕ = 1.0 are shown in Fig. 4 for the five injector blocks tested. Since the divergence angle downstream of x = 576 mm for these runs were zero, the exit stream did not separate as evidenced by the distributions. Beyond x = 160 mm, there is no significant difference in the distributions among the models, showing almost the same degree of heat release up to this region. In the constant area section of $x > 576$ mm, p_w gradually increases downstream.

The peak pressure p_{max}, normalized with the wall pressure p_{wa}, at the point where p_w diverged from the noninjection case, is cross plotted from Figs. 3 and 4 against the relative increment of total enthalpy $\delta h_t/h_{ta}$ in Fig. 5. Figure 5a is for model N1 at various ϕ and T_{ta}. Except for T_{ta} = 1000 K, the data correlate fairly well with $\delta h_t/h_{ta}$. A similar attempt was made to correlate them with ϕ/T_{ta} or $\delta T_t/T_{ta}$, which is recommended as governing parameters at NASA Langley[12] and JHU-APL,[7] respectively. However, these parameters did not show as good a correlation as the present one. In the figure, pressures behind the step calculated by applying Billig's model[3] are also shown as solid curves for comparison. They are considerably lower than the present results, but the qualitative tendency, i.e., a relatively higher pressure level at T_{ta} = 1000 K compared with those at the other T_{ta}, is similar. With the same entrance Mach number and combustor geometry as in the model presented here, a general expression for p_{max}/p_{wa} may be expressed as the following equation:

$$p_{max}/p_{wa} = f(\gamma, W) \cdot \delta h_t/h_{ta} \qquad (5)$$

Therefore, the exceptional trend of the case with T_{ta} = 1000 K may be due to the effects of differences in molecular weight and specific heat ratio of vitiated air at the combustor entrance, which seems to be less sensitive at higher T_{ta}.

Figure 5b compares p_{max}/p_{wa} for the other models at T_{ta} = 2000 K with the data in Fig. 5a. Model N3 has the lowest and model N1 has the highest peak pressures among the injector blocks tested. This shows the strong effect of the constant area length on the combustor performance, as pointed out in

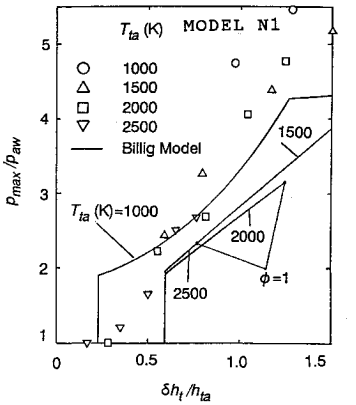

a) Model N1

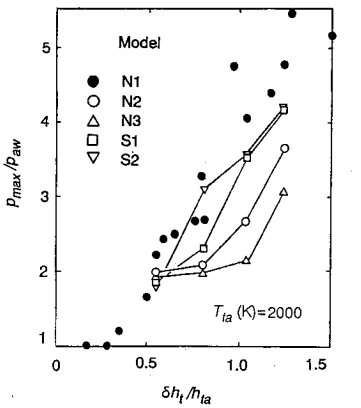

b) T_{ta} = 2000 K

Fig. 5 p_{max} vs $\delta h_t/h_{ta}$.

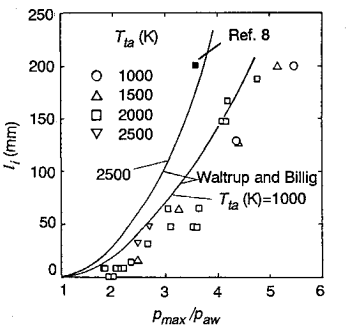

Fig. 6 Peak pressure and upstream influence.

previous investigations.[2,8,11,19] The swept-step model S1 shows a slightly lower peak pressure compared with model N1. However, the reversed swept-step model S2 exhibits almost the same distribution as model N1, i.e., there is no appreciable peak pressure reductions from model N1. It can be stated from these results that the effect of the sweep of the step is not significant compared with that due to reduction of the length of constant area section such as in model N3, despite our expectation implied by the data of Anderson et al.[1]

Although not shown here, similar tendencies were obtained between $\delta h_t/h_{ta}$ and the distance from the step to the point where the effect of combustion reached the upstream area, implying that the latter is correlated with p_{max}/p_{wa}. Such a correlation is shown in Fig. 6 for all the present data. The l_i, is defined as that along the x axis from the step to the point where the wall pressure diverges from the noninjection case. A fairly good correlation can be seen, irrespective of both T_{ta} and the injector geometry. Solid curves drawn in the figure are based on an empirical correlation derived by Waltrup and

Billig.[5] This was taken from an experiment on supersonic flow in a circular cross-section duct without step, and its validity for a rectangular duct was also confirmed recently.[7] In applying this empirical relation to the present experiment, the momentum thickness of the boundary layer was set to be 0.1 mm based on the Pitot profile measurement as described earlier.

The empirical curves predict higher peak pressure and show strong dependency on T_{ta} compared with the present data, implying that a correction term accounting for the effect of T_{ta} needs to be incorporated into their model. It should be noted, however, that their empirical curves are based on the distance from the point of peak pressure, not from the step as in the present data. As can be seen in Figs. 3 and 4, the former point was located downstream of the latter by up to 20 mm. Even considering the difference in this distance, their empirical curves lie still higher than the present data. Another datum point from our experiment on a circular cross-section combustor with fuel injected upstream of the step[9] is also shown in the figure. It shows a higher peak pressure than the present data, too. These arguments indicate an important role of backward-facing steps, i.e., suppression of combustion-induced pressure waves. It should furthermore be noted that the steps can act as a damper for the pressure waves by reducing their magnitude. However, the step may cause inefficient combustion by making static pressure lower,[19] requiring a sort of compromise.

Cross-Sectional Distributions

Contours of the local fuel equivalence ratio ϕ' at the hypothetical state before burning over the exit cross section of various combustor lengths for model N1 are shown in Fig. 7. Arrows along the boundaries of each cross section show the corresponding locations of the fuel injection orifices located upstream of the section presented. Although narrow regions of high concentration of fuel near the top and bottom walls can be seen in the shortest combustor, fuel jets seem to coalesce quite early as evidenced by the disappearance of traces of each fuel jet. A region of high fuel concentration in the central part of the cross section still remains even in the longest combustor, showing very slow mixing because of the coalescence of the fuel jets.

The effects of L_c and ϕ on ϕ' contours are shown in Fig. 8. The combustor lengths L are 336 mm for model N1 and 262 mm for N3 (198-mm downstream of the exit of the injector block in both cases). Fuel jet traces can be identified in model N1 with $\phi = 0.6$ and in model N3 with $\phi = 1.0$. For model N1, another experiment was also conducted with fuel injected from only one of the side walls. In this run ϕ was set equal to 0.5 to match the injection condition with that in Fig. 7. The results for this case at $x = 336$ mm (Fig. 9) exhibited traces of the fuel jets clearly, and the fuel jets penetrated to a point near the center of the duct.

It has been experimentally confirmed that penetration of the perpendicular jet into a supersonic mainstream increases with a decrease in its dynamic pressure[20,21] and with an increase in boundary-layer thickness[22] at the point of injection. The value of the dynamic pressure behind a shock wave does not necessarily increase with the shock strength, but rather decreases when the latter is high. Therefore, it is quite possible that the dynamic pressure decreased with the increase in shock strength in the present run, contrary to the conclusion derived at NASA Langley.[17,23,24] Furthermore, the boundary layer is presumably disturbed and thickened by the precombustion shock. In addition, it is anticipated from the experimental results of supersonic mixing layers[25] that the jet issuing into a coflowing mainstream spreads more rapidly when the Mach number of the latter is lowered by a shock wave as in the present experiment.

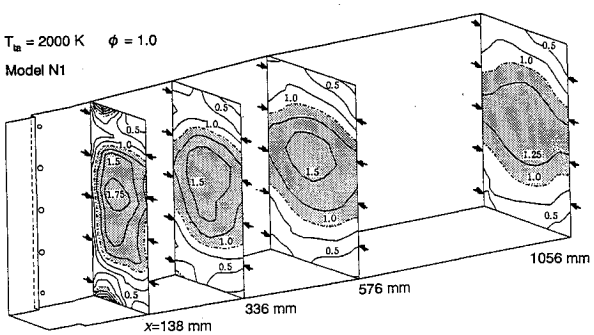

Fig. 7 Variation of local equivalence ratio contours for the model N1.

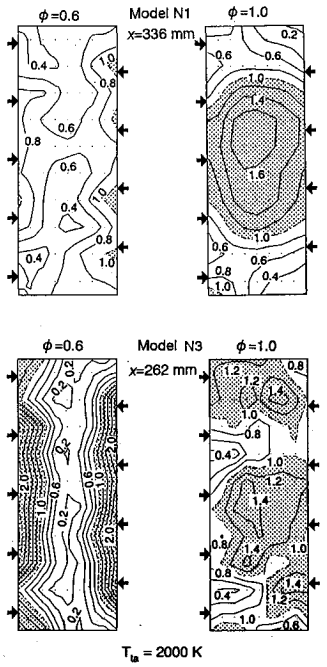

Fig. 8 Effects of L_c and ϕ on ϕ' contours.

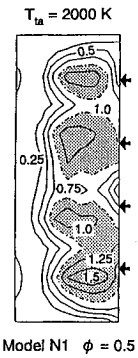

Fig. 9 Contours of ϕ' with injection from one wall only.

Considering these experimental evidences and arguments, the above results can be explained as follows: The fuel injected in model N1 with $\phi = 1.0$ (Fig. 7) may have penetrated much deeper than those with $\phi = 0.6$ (upper left in Fig. 8), that injected from only one wall (Fig. 9), and that in model N3, because of stronger precombustion shock and a thicker boundary layer. As described earlier with regard to the wall pressure distributions, the length of the constant area section has a strong effect on the strength of the precombustion shock. This may have been responsible for the difference in mixing pattern between models N1 and N3 seen in Fig. 8. The deeper penetration and faster spreading of the fuel jets in model N1 with $\phi = 1.0$ show there was rapid mixing very near the injection orifices, followed, however, by its suppression downstream due to coalescence of the fuel jets. On the other

hand, for model N3 with $\phi = 1.0$ and model N1 with $\phi = 0.6$, the precombustion shock was weakened by a shorter constant area section in the former, and by lower heat release in the latter, causing the traces of the fuel jets to survive for a longer distance. For $\phi = 0.6$ with model N3 (lower left in Fig. 8), the injected fuel is stratified because of much weaker penetration of fuel jets. It should be noted from Figs. 7 and 8 that the mixing performance is very sensitive to both L_c and ϕ.

In the experimental results at NASA Langley,[17,23,24] there are clearly identifiable traces of the fuel jets. This is due to their shorter constant area section ($L_c/H = 0.65$ and 1.22 compared with the present value of 3.0 of model N1) and the larger divergence angle (half-angle of 2.0–6.6 deg compared with the present 1.7 deg) of the combustor. It seems probable that the strength of the precombustion shock may depend not only on the magnitude of the combustion-induced heat release, but also its gradient. Therefore, the fact that the fuel injection orifices on the walls opposing each other were axially staggered in their experiments as in the present N2 model, also accounts for this difference, because such staggering can relax the heat release gradient in the x direction. The peak pressure ratio p_{max}/p_{wa} in their experiment was 2.0 at the highest, compared with the present 4.5 in model N1, supporting the above reasoning.

The ϕ' contours for model N2 shows just the intermediate characteristics between models N1 and N3, and those of models S1 and S2 have a pattern similar to that of model N1 with partial evidence of fuel jet traces. These results are not shown here.

Combustor Performances

Figure 10 shows variations of η_c with L/H for all the models with $\phi = 1.0$ and $T_{ta} = 2000$ K. Combustion efficiencies over 70% are attained for L less than $5H$, but their growth rate with L is so small that they do not seem to exceed 90%, even with a combustor longer than those in the present test. Though the difference is slight, model N1 shows the worst efficiency, whereas models N2 and N3 attained the best performances for the range of combustor lengths tested. The lowest η_c in model N1 may be due to the aforementioned coalescence of the fuel jets, which prevented further progress of fuel-air mixing. In this case, however, it should be noted again that the fuel penetration and mixing rate may be higher, and therefore, higher mixing and combustion efficiencies may have been attained at a very early stage after fuel injection, as mentioned previously. The highest η_c in models N2 and N3 may be primarily due to a shorter constant area section, leading to survival of the fuel jet traces, which allows further mixing. Contrary to the case with model N1, however, fuel penetration and mixing rate may be lower near the fuel injection orifices. These phenomena can be regarded as evidence of the important role of the injector geometry, especially the length of the constant area section, in supersonic combustion.

The swept-step models, S1 and S2, show a slightly better η_c than the unswept model N1. However, there is no clear difference in η_c between models S1 and S2. Again, despite our expectation, reversing the opposing swept-steps with each other is found to have no advantage over the nonreversed case with regard to wall pressure distributions. The mixing efficiency, though not shown here, had similar characteristics and almost the same magnitude as η_c.

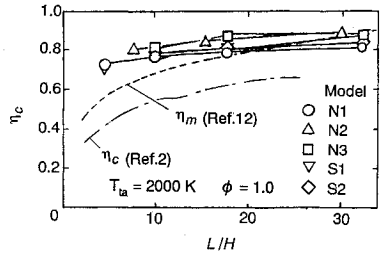

Fig. 10 Combustion efficiencies.

Also shown in Fig. 10 are NASA-Langley's data of an experimentally obtained combustion efficiency[2] as a dotted curve and of an empirical correlation for the mixing efficiency[12] as a dot-dashed curve. Note that their mixing correlation was obtained from a nonreacting experiment. They are quite lower than the present results for $L < 10H$, but the mixing correlation overcomes the present results at $x = 30$–$40H$, where the growth rate of η_c in the present results is very small. As explained previously, these differences are due to a smaller L_c, a larger divergence angle, and axially staggered fuel injectors in the combustor model used at Langley as compared with those in the present one. These differences may have resulted in the strengths of precombustion shocks being different from each other.

Summarizing the effect of the length of the constant area section on the combustor performance again, it can be stated that a larger L_c is very effective for enhancing mixing between air and the fuel, but care must be taken to avoid coalescence of fuel jets, which suppresses further mixing. Therefore, there must be an optimum value of L_c giving the best mixing performances. Further insight into the best way to adjust diameter, axial, or transversal locations, spacing of fuel injection orifices, injection conditions, and the geometry of the injector is required for optimization of combustor design.

Conclusions

Results of an experiment on the effect of fuel injector geometry on scramjet combustor performance with an entrance Mach number of 2.5 were presented. The following observations can be made:

1) The injector model with the shortest constant area section had the lowest peak pressures while that with the longest one had the highest.

2) The swept-step model showed a slightly lower peak pressure compared with that of the unswept model with the same effective constant area section.

3) The reversed swept-step model exhibited almost the same wall pressure distribution as the unswept model.

4) The peak wall pressure and the distance of upstream influence measured from the step correlated well irrespective of both the air total temperature and the injector geometry.

5) An empirical model derived by Waltrup and Billig[5] predicted a longer upstream influence than the present data at the same peak pressure. This, together with the authors' previous experimental results, accounts for the suppression of the upstream propagation of combustion-induced pressure waves by the rearward-facing step.

6) The injector model with the longest constant area section at the fuel equivalence ratio of unity caused coalescence of fuel jets at a very early stage downstream of the injection. Such a coalescence did not occur when the fuel equivalence ratio was decreased to 0.6 or when models with a shorter constant area section were used. This high sensitivity of fuel mixing to the length of the constant area section is due to pressure and Mach number changes.

7) The combustion efficiency is the highest for the injector model with the shortest constant area section, whereas that with the longest one has the lowest, depending on whether coalescence of fuel jets occurs or not.

8) The swept-step and reversed swept-step models show a slightly higher combustion efficiency compared with the unswept model of the same effective constant area section.

9) Reversing the steps opposing each other did not show any advantage in the mixing and combustion efficiencies.

10) The present injectors showed much higher combustion efficiencies than those obtained at NASA Langley near the injection orifices, owing to the shorter constant area section, smaller divergence angle, and axially nonstaggered arrangement of the injection orifices. Downstream of the combustor,

however, the growth rate of mixing becomes decreased and the present data were overcome by the Langley's mixing correlation.

Other important results not directly concerned with the effect of the injector geometry are as follows:

11) Values of the peak wall pressure and the distance of the upstream influence correlate well with the relative increment of the total enthalpy caused by combustion, except at the vitiated air total temperature of 1000 K, where effects of molecular weight and specific heat ratio become significant. Similar correlation utilizing the fuel equivalence ratio divided by total temperature or relative increment of total temperature instead of the relative enthalpy was less successful.

12) Billig's one-step model[3] agreed qualitatively well with the effect of vitiated air total temperature on the peak pressure, but predicted relatively lower values.

Acknowledgment

The authors express their gratitude to Akio Moro, senior researcher at the National Aerospace Laboratory, Kakuda Research Center, for providing a computer program of chemical equilibrium calculations.

References

[1]Anderson, G. Y., Reagon, P. A., Gooderum, P. G., and Russin, W. G., "Experimental Investigation of a Swept-Strut Fuel Injector Concept for Scramjet Application," NASA TN D-8454, Aug. 1977.

[2]Diskin, G. S., and Northam, G. B., "Effects of Scale on Supersonic Combustor Performance," AIAA Paper 87-2164, June 1987; see also ICAS Paper 88-2.1.4, 1988.

[3]Billig, F. S., and Dugger, G. L., "The Interaction of Shock Waves and Heat Addition in the Design of Supersonic Combustors," *Proceedings of 12th Symposium (International) on Combustion*, Combustion Inst., Pittsburgh, PA, 1969, pp. 1125–1134.

[4]Billig, F. S., Dugger, G. L., and Waltrup, P. J., "Inlet-Combustor Interface Problems in Scramjet Engines," 1st International Symposium on Air Breathing Engines, Marseille, France, June 1972.

[5]Waltrup, P. J., and Billig, F. S., "Prediction of Precombustion Wall Pressure Distribution in Scramjet Engines," *Journal of Spacecraft and Rockets*, Vol. 10, No. 9, 1973, pp. 620–622.

[6]Waltrup, P. J., and Billig, F. S., "Structure of Shock Waves in Cylindrical Ducts," *AIAA Journal*, Vol. 11, No. 9, 1973, pp. 1404–1408.

[7]Bement, D. A., Stevens, J. R., and Thompson, M. W., "Measured Operating Characteristics of a Rectangular Combustor/Inlet Isolator," AIAA Paper 90-2221, July 1990.

[8]Masuya, G., Chinzei, N., Kudou, K., Murakami, A., Komuro, T., and Ishii, S., "A Study of Air Breathing Rockets (3)—Supersonic Mode Combustors" (in Japanese), National Aerospace Lab., NAL TR-756, Tokyo, Japan, April 1983.

[9]Komuro, T., Murakami, A., Kudou, K., Masuya, G., and Chinzei, N., "An Experiment on a Cylindrical Scramjet Combustor (1) Simulated Flight Mach Number of 4.4" (in Japanese), National Aerospace Lab., NAL TR-918, Tokyo, Japan, Nov. 1986.

[10]Komuro, T., Murakami, A., Kudou, K., Masuya, G., and Chinzei, N., "Experiment on a Cylindrical Scramjet Combustor (2) Simulated Flight Mach Number of 6.7" (in Japanese), National Aerospace Lab., NAL TR-969, Tokyo, Japan, March 1986.

[11]Avrashkov, V., Baranovski, S., and Levin, V., "Gasdynamic Features of Supersonic Kerosene Combustion in a Model Combustion Chamber," AIAA Paper 90-5268, July 1990.

[12]Northam, G. B., and Anderson, G. Y., "Supersonic Combustion Ramjet Research at Langley," AIAA Paper 86-0159, Jan. 1986.

[13]Sato, Y., Sayama, M., Masuya, G., Komuro, T., Kudou, K., Murakami, A., Tani, K. and Chinzei, N., "Experimental Study on Autoignition in Scramjet Combustor," *Journal of Propulsion and Power*, Vol. 7, No. 5, 1989, pp. 657–658.

[14]Sato, Y., Sayama, M., Ohwaki, K., Masuya, G., Komuro, T., Kudou, K., Murakami, A., Tani, K., Wakamatsu, Y., Kanda, T., Chinzei, N., and Kimura, I., "Effectiveness of Plasma Torches for Ignition and Flameholding in Scramjet," *Journal of Propulsion and Power* (to be published).

[15]Masuya, G., Kudou, K., Murakami, A., Komuro, T., Tani, K., Kanda, T., Wakamatsu, Y., and Chinzei, N., "Some Governing Parameters of Plasma Torch Igniter/Flameholder in Scramjet Combustor," AIAA Paper 90-2098, July 1990.

[16]Murakami, A., Komuro, T., Kudou, K., Masuya, G., and Chinzei, N., "An Air Heater for Scramjet Test" (in Japanese), National Aerospace Lab., NAL TR-912, Sept. 1986.

[17]Anderson, G. Y., Eggers, J. M., Waltrup, P. J., and Orth, R. C., "Investigation of Step Fuel Injectors for an Integrated Modular Scramjet Engine," *Proceedings of 13th JANNAF Combustion Meeting*, CPIA 281, Laurel, MD, Sept. 1976, pp. 175–189.

[18]Guy, R. W., and Mackley, E. A., "Initial Wind Tunnel Tests at Mach 4 and 7 of Hydrogen-Burning, Airframe-Integrated Scramjet," *Proceedings of the 4th International Symposium on Air Breathing Engines*, AIAA, New York, April 1979, pp. 347–358.

[19]Waltrup, P. J., Dugger, G. L., Billig, F. S., and Orth, R. C., "Direct-Connect Tests of Hydrogen-Fueled Supersonic Combustors," *Proceedings of 16th Symposium (International) on Combustion*, Vol. 3, Combustion Inst., Pittsburgh, PA, Dec. 1976, pp. 1619–1629.

[20]Zuboski, E. E., and Spaid, F. W., "Secondary Injection of Gases into a Supersonic Flow," *AIAA Journal*, Vol. 2, No. 10, 1964, pp. 1689–1696.

[21]Orth, R. C., Schetz, J. A., and Billig, F. S., "The Interaction and Penetration of Gaseous Jets in Supersonic Flow," NASA CR-1386, July 1969.

[22]McClinton, C. R., "Effect on Ratio of Wall Boundary-Layer Thickness to Jet Diameter on Mixing of a Normal Hydrogen Jet in a Supersonic Stream," NASA TM X-3030, June 1974.

[23]Eggers, J. M., Reagon, P. G., and Gooderum, P. B., "Combustion of Hydrogen in a Two-Dimensional Duct with Step Fuel Injectors," NASA TP-1159, May 1978.

[24]McClinton, C. R., "Interaction Between Step Fuel Injectors on Opposite Walls in a Supersonic Combustor Model," NASA TP-1174, May 1978.

[25]Chinzei, N., Masuya, G., Komuro, T., Murakami, A., and Kudou, K., "Spreading of Two-Stream Supersonic Mixing Layers," *Physics of Fluids*, Vol. 29, No. 5, 1986, pp. 1345–1347.